PTFE−Polystyrene Core−Shell Nanospheres and Nanocomposites

Elena Giani, Katia Sparnacci, and Michele Laus*

Dipartimento di Scienze e Tecnologie Avanzate, Corso Borsalino 54, Università del Piemonte Orientale "A. Avogadro", INSTM, UdR Alessandria, 15100 Alessandria, Italy

Giovanna Palamone, Valeri Kapeliouchko, and Vincenzo Arcella

Solvay Solexis SpA, Piazzale Donegani 5/6, 15047 Spinetta Marengo, Alessandria, Italy

Received December 20, 2002; Revised Manuscript Received April 11, 2003

ABSTRACT: PTFE latexes with particles in the submicrometer size range were employed as seeds in the emulsifier-free styrene emulsion polymerization to obtain PTFE−polystyrene (PS) core−shell nanospheres. Stable latexes were generally obtained. Neither residual PTFE nor secondary nucleation was observed, thus leading to PTFE−PS core−shell latexes. By appropriately choosing the ratio between the styrene monomer and the PTFE seed in the reaction mixture, it is possible to obtain spheres with predetermined sizes and narrow size distribution. In all cases, a slightly hemispherical morphology was observed. Peculiar effects related to the high degree of segregation of PTFE cores and their small size, and possibly to the PTFE/PS interface, were observed.

Introduction

Fluorinated polymers are particularly attractive and versatile compounds because of their unique combination of properties linked to the low polarizability and the strong electronegativity of the fluorine atom.[1,2] Fluoropolymers exhibit high thermal, chemical, aging, and weather resistance, excellent inertness to solvents, hydrocarbons, acids, and alkalis, low dielectric constants, low flammability, low refractive index, low surface energy and moisture adsorption, and interesting oil and water repellency. Consequently, these polymers, among them poly(tetrafluoroethylene) (PTFE), have found major developments in modern technologies with applications ranging from building, automotive, and aerospace industries to optics and microelectronics. However, the most common way of tailoring material properties by blending is very hard to bring about successfully because of the inherently low adhesion of the fluoropolymers, which results in low dispersion degrees within the matrix and unefficient mechanical coupling between the various blend components. Several studies were addressed to the surface modification of PTFE using chemicals, grafting, sputtering, and also plasma treatments.[3]

An alternative approach could be represented by the preparation of composites starting from core−shell architectures in which the core is constituted by a fluorinated polymer and the shell by a conventional polymer.[4] If the glass transition of the latter polymer is lower than the one of the fluoropolymer, annealing the material at a temperature intermediate between the two glass transitions, but sufficiently high to ensure that the flow of the shell-forming polymer fills the voids, would lead to the formation of a continuous polymer matrix in which the cores are arranged in regular registry. Since the characteristic size of the different domains is in the nanometer range, much smaller than the wavelength of light, the material should be optically transparent. Such a multiphasic nanostructured composite can be of interest in nanophotonics.[5,6] In fact, in these systems optical scattering should be very low due to the very small size of the PTFE particles which can be prepared with sizes smaller than 20 nm.

Ausimont (now Solvay Solexis) developed[7,8] the tetrafluoroethylene (TFE) homo- and copolymerization microemulsion technology, on industrial scale, based on the use of perfluoropolyethers (PFPE) in oil/water microemulsion. Poly(tetrafluoroethylene) (PTFE) aqueous dispersions can be obtained, with particle concentration number as high as $10^{18}-10^{19}$ and particle size as small as 10 nm. Moreover, by varying the amount and type of PFPE as well as the quantity and nature of the comonomers, PTFE particles with a great morphological diversity can be obtained. The resulting PTFE nanoparticulate is presently employed in a variety of applications[9−11] including components in PTFE bimodal mixtures, ultralow-K dielectric materials, nanofillers for fluoroelastomers, and fire retardant additives with the reported purpose of inhibiting the dripping of molten particles from the burning polymer.

For the latter application, a perfect degree of dispersion of the core−shell nanoparticles within a polymer matrix could be obtained if the shell is constituted by the same polymeric material with which the polymer matrix is made up, thus leading to a novel class of highly specific but very efficient PTFE-based additives.

In the present study, some of the above PTFE latexes, marked MD, DV2, and DV3, with particles in the submicrometer size range, are employed as seeds in the emulsifier-free styrene emulsion polymerization thus leading to PTFE−PS core−shell nanospheres. Very few data can be found in the literature concerning the preparation and physicochemical characteristics of PTFE based core−shell particles. In particular, several composite particles consisting of PTFE core and cross-linked polybutadiene shell were described by Okaniwa,[12] whereas the preparation of one sample only of core−shell particles in which the core is made up of PTFE and the shell of cross-linked PS was reported by Othegraven.[13] In addition, through grafting reactions of hydrocarbon monomers on preirradiated PTFE, core−

* Corresponding author: Telephone: +390131287433. Fax: +390131287416. E-mail: laus@mfn.unipmn.it.

10.1021/ma0259970 CCC: $25.00
Published on Web 05/20/2003

Table 1. PTFE Latex Characteristics

sample	shape	*d* (nm)	free surfactant (M)	solid (g/L)	no. of particles L^{-1}	conductivity (μS/cm)
MD	sphere	41		347.6	3.1×10^{18}	860
DV2	sphere	33	0.025	358.3	6.8×10^{18}	1980
DV3	rodlike	62	0.038	294.5	1.2×10^{18}	1930
MDd	sphere	41		264.1	2.1×10^{18}	280
DV2d	sphere	33		243.5	4.5×10^{18}	460
DV3d	rodlike	62		211.3	8.2×10^{17}	415

shell nanoparticles consisting of a PTFE core and a thin PMMA shell, were prepared in CO_2/aqueous system.[14]

Experimental Section

Materials. Styrene (99%) was purchased from Aldrich and washed with 3 × 100 mL of 1.0 M sodium hydroxide, 3 × 100 mL of water, dried with anhydrous sodium sulfate, and stored at 5 °C. Potassium persulfate (Carlo Erba, 98%) was used without further purification.

Preparation of the PTFE Latex. Three PTFE latexes, MD, DV2, and DV3, were provided from Solvay Solexis. They were synthesized through miniemulsion polymerization of tetrafluoroethylene TFE stabilized with a fluorinated anionic surfactant **1**, having the following structure

$$ClC_3F_6O(C_3F_6O)_nCF_2COO^-Na^+$$
1

wherein *n* is such as to give an acidimetric molecular weight equal to 547, and with a perfluoropolyether **2**, having a structure of the type

$$R_fO(C_3F_6O)_{n'}(CF_2O)_{m'}R'_f$$
2

where R_f and R'_f equal to or different from each other are perfluoroalkyls from 1 to 3 carbon atoms, and *n′* and *m′* are integers such as to give a number-average molecular weight of about 700. These products are commercially available from Solvay Solexis under the trade names Galden and Fomblin.

As a typical example, the preparation of MD latex was reported. First, 3000 g of **1** and 1800 g of **2** were added to 4800 g of water to obtain a perfectly clear microemulsion in the temperature range between 2 and 46 °C. Then 9500 g of this microemulsion, equal to 2970 g of **1** and 1780 g of **2**, and 2000 g of paraffin, with softening point of 52−54 °C, are combined with 275 L of degassed water in a 400 L stainless steel water-jacketed reactor equipped with mechanical stirrer and previously put under vacuum (−660 mmHg). The stirring was started, and 1200 g of perfluorodioxole were added. Then the reactor was pressurized at 20 bar with C_2F_4, the temperature was set to 90 °C, and 1500 mL of an ammonium persulfate solution at a concentration of 43.8 mM were fed into the reactor. The pressure was maintained at 20 bar by feeding C_2F_4 until 120 000 g reacted. The reactor was then depressurized and cooled, and a polymer dispersion was finally downloaded. The latexes produced by the above procedure are stable colloidal dispersions of PTFE in water. DV2 latex was prepared in the same way starting from 18 800 g of the microemulsion, equal to 5900 g of **1** and 3500 g of **2**, and feeding 88 000 g of C_2F_4, whereas latex DV3 was prepared starting from 24 000 g of the microemulsion, equal to 7500 g of **1** and 4500 g of **2** and feeding 88 000 g of C_2F_4. In addition, all these latexes were thoroughly dialyzed using a semipermeable membrane to reduce the concentration of free surfactant leading to latexes MDd, DV2d, and DV3d. The latex characteristics, including the solid content, the particle number concentration, and the conductivity are collected in Table 1. Particle average diameters were determined by Photon Correlation Spectroscopy.

Preparation of PTFE/PS Core—Shell Nanospheres. The PTFE−PS core−shell latexes were synthesized by emulsifier-free batch-seeded emulsion polymerization with PTFE seed particles. All the polymerizations were carried out in a 1 L five-neck reactor at 75 °C equipped with a condenser, a mechanical stirrer, a thermometer, and inlets for nitrogen and styrene. The appropriate amount of PTFE latex was introduced into the reactor containing 500 mL of deionized water at room temperature with a stirring rate of 300 rpm. The mixture was purged with nitrogen and nitrogen was fluxed during the entire polymerization procedure. The mixture was then heated to 75 °C, and styrene (70.0 mL, 0.612 mol) was added. After additional 15 min equilibration time, a potassium persulfate aqueous solution (10 mL, 0.74 mmol) was added and the mixture was reacted for 24 h. The obtained latex was purified from the unreacted monomer by repeated dialyses. All the PTFE/PS latexes were obtained following the above general procedure by varying the initial PTFE latex amount. Table 2 collects the details of the various preparations, including the latex yield and solid content.

Table 2. Yield and Solid Content of the Samples

PTFE latex	series	sample	% PTFE latex	yield (%)	solid content (g/mL)
		3MDS	3	76.4	0.1121
MD	MDS	6MDS	6	77	0.1128
		12MDS	12	83	0.065
		18MDS	18	81.7	0.1247
MDd	MDdS	3MDdS	3	83	0.1068
		6MDdS	6	86	0.1161
		3DV2S	3	94.5	0.1138
DV2	DV2S	6DV2S	6	81.3	0.1088
		12DV2S	12	72.8	0.0673
		18DV2S	18	70.4	0.1101
		3DV2dS	3	72.3	0.0997
DV2d	DV2dS	6DV2dS	6	59.1	0.1032
		12DV2dS	12	68	0.1026
		18DV2dS	18	65	0.0958
DV3	DV3S	3DV3S	3	65	0.0711
		3S	3	85	0.1019
	S	6S	6	75	0.0885
		12S	12	86.8	0.0943
		18S	18	82.3	0.0876

Preparation of PS Latexes. Some PS latexes were synthesized by emulsion polymerization using the perfluoropolyether surfactant (PFPE) mixture at the same concentration estimated to be present in the polymerizations performed in the presence of the DV2 latex in variable amounts. All these polymerizations were carried out in a 1 L five-neck reactor at 75 °C equipped with a condenser, a mechanical stirrer, a thermometer, and inlets for nitrogen and styrene. The appropriate amount of a 0.025 M solution of PFPE in water was introduced into the reactor containing 500 mL of deionized water at room temperature with a stirring rate of 300 rpm. The mixture was purged with nitrogen, and nitrogen was fluxed during the entire polymerization procedure. The mixture was then heated to 75 °C, and styrene (70.0 mL, 0.612 mol) was added. After additional 15 min of equilibration time, a potassium persulfate aqueous solution (10 mL, 0.74 mmol) was added, and the mixture was reacted for 24 h. The obtained latex was purified from the unreacted monomer and residual surfactant by repeated dialyzes. All the PS latexes were obtained following the above general procedure by varying the volume of the PFPE solution leading to sample 3S-18S corresponding to 11.5, 23.0, 46.0, and 69.0 mL of the 0.025 M PFPE solution.

Characterization. The concentration of latex dispersion was determined gravimetrically. Particle size and size distribution were measured by transmission electron microscope (TEM) and by dynamic light scattering. TEM images were obtained using a Philips CM10. The diluted samples were mounted on 400-mesh carbon-coated copper grids and left to dry. The TEM photographs were digitalizated and elaborated by the Scion Image processing program. From 100 to 150 individual microsphere diameters were measured for each sample. Dynamic light-scattering analysis was performed at 25 °C, with a Malvern Zetasizer 3000 HS at a fixed scattering

angle of 90°, using a 10 mV He−Ne laser and PCS software for Windows (version 1.34, Malvern, U.K.). Each value is the average of four measurements. The instrument was checked with a standard polystyrene latex with a diameter of 200 nm. Electrophoretic mobility was measured with a Malvern Zetasizer 3000 HS. Each value is the average of five measurements. The instrument was checked using a latex with known ζ-potential. Average molar masses were determined by SEC of THF solutions with a 590 Waters chromatograph equipped with refractive index and ultraviolet detectors, using PLgel 10^3, 10^4, 10^5, and 10^6 Å columns calibrated with PS standard samples. For the determination of the PS molar masses, 1.0 mL of THF was added to about 100 mg of the core−shell sample. After centrifugation at 18 000 rpm for 20 min, quantitative sedimentation of the PTFE was obtained. Then supernatant was withdrawn and the solvent evaporated under reduced pressure.

Thermogravimetric analysis (TGA) was performed with a Rheometric TGA thermobalance at a scanning rate of 10 °C/min from room temperature up to 800 °C under nitrogen flow. Differential scanning calorimetry (DSC) was carried out using a Mettler-Toledo DSC 821 apparatus. Samples of about 5 mg were employed. The instrument was calibrated with high purity standards (indium, naphthalene, benzoic acid, cyclohexane) at 10 °C·min^{-1}. Dry nitrogen was used as purge gas. The samples for the dynamic-mechanical analysis were prepared introducing the powder polymer sample into a rectangular mold. The entire assembly was then placed between press plates with a nominal pressure of 4.9×10^7 Pa and allowed to stand at room temperature for 20 min. The temperature was then raised to 160 °C and the pressure released to 4.9×10^6 Pa. After 15 min, the sample was quenched into cold water and recovered as rectangular $20 \times 5 \times 2$ mm sheets. The modulus was measured with a dynamic mechanical analyzer Rheometric DMTA V, employing the single cantilever flexural geometry. A static-to-dynamic stress ratio of 120% and a scanning rate of 4 °C/min were chosen. The strain was sufficiently small to be within the linear viscoelastic range.

Results and Discussion

PTFE MD and DV2 latexes consist of spherical particles of 41 and 33 nm whereas DV3 consists of rodlike particles with an equivalent radius of 62 nm and an axial ratio of 3.2. These latexes contain residual PFPE surfactant which contributes to the latex stability. However, as the presence of the residual surfactant could interfere with the successive emulsifier-free seeded styrene emulsion polymerization, all the PTFE latexes were dialyzed to reduce the residual surfactant amount thus leading to latexes MDd, DV2d, and DV3d, with d standing for dialyzed. The physicochemical characteristics of the PTFE latexes before and after dialysis are collected in Table 1.

The emulsifier-free seeded styrene emulsion polymerizations were performed by adding appropriate amounts of the PTFE latex and styrene into deionized water and running the reactions at 75 °C for 24 h using potassium persulfate as the free radical source. At the end of the reaction, the latexes were purified from the unreacted monomer by repeated dialyses. In all the polymerization reactions, the styrene and potassium persulfate amounts as well as the water content were kept constant whereas variations were allowed in the PTFE latex amount. Starting from the six latexes, namely MD, DV2, and DV3 and their dialyzed counterparts, and changing the ratio between the PTFE latex and styrene, six sample series were obtained marked *n*MDS, *n*DV2S, *n*DV3S, *n*MDdS, *n*DV2dS, and *n*DV3dS, where *n* represents the initial PTFE volume percent with respect to styrene, MD, DV2, DV3, MDd, DV2d, and DV3d, indicate the PTFE latex employed, and S stands for styrene.

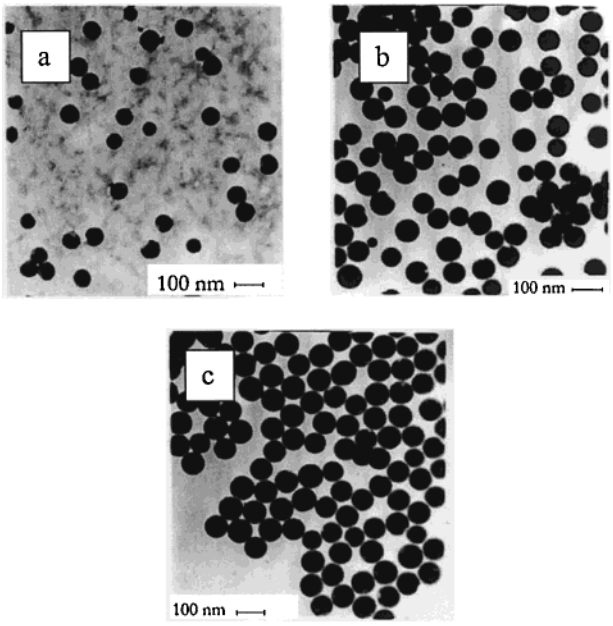

Figure 1. TEM micrographs of sample 6MDS at different reaction time: (a) 30 min; (b) 1.5 h; (c) 3 h.

In addition, a series of PS latexes were synthesized by emulsion polymerization using the perfluoropolyether surfactant (PFPE) mixture at the same concentration estimated to be present in the DV2 latex. This PS sample series was marked *n*S in analogy with the corresponding *n*DV2S series.

The colloidal stability of the latexes deriving from DV3, DV3d, and MDd is very small. Only three relatively stable latexes, namely 3DV3S, 3MDdS, and 6MDdS, were obtained. For all the other compositions, latex coalescence was observed immediately after the beginning of the polymerization. In contrast, stable latexes were obtained from the latexes deriving from MD, DV2, and DV2d with nanosphere yields ranging from 65 to 95% and nearly quantitative styrene conversions (Table 2).

Figure 1 reports TEM micrographs of sample 6MDS taken at different reaction times. After 30 min, the system is constituted by a great number of PTFE nanoparticles which appear gray and not well resolved and a few black and bigger nanospheres with an average diameter of about $d = 90$ nm deriving from the styrene polymerization. After 1 h, the number of gray particles decreases with respect to the black ones. In addition, the size of the latter nanospheres increases (average diameter $d = 115$ nm). After 3 h, the gray particles practically disappear, and the sample consists of black nanospheres only with diameter of about $d = 118$ nm.

Figures 2 and 3 report the PCS spectrum and a TEM micrograph, respectively, of sample 6MDS after 24 h reaction time. For comparison, the PCS curve of the MD latex and the micrograph of the purely PS sample 6S are reported in Figures 2 and 3, respectively. No residual PTFE deriving from MD latex is present, thus indicating that PTFE is highly efficient as seed in the styrene polymerization. In addition, the monomodal and very narrow size distribution of sample 6MDS suggests that styrene polymerization occurs quantitatively onto the PTFE seeds and no secondary nucleation occurs. This conclusion is also supported by TEM analysis.

Sample 6S is constituted by nanospheres with regular shape whereas nanospheres 6MDS appear to have a

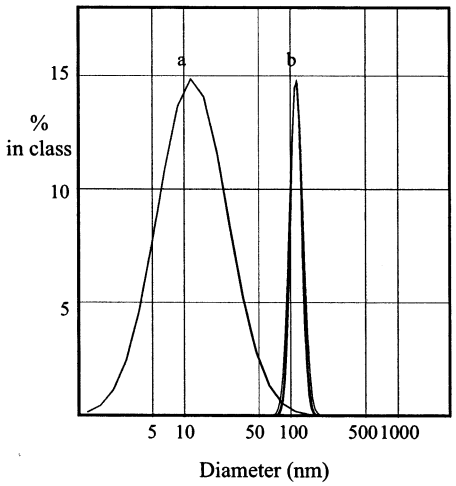

Figure 2. PCS spectrum of latex MD (a) and sample 6MDS (b).

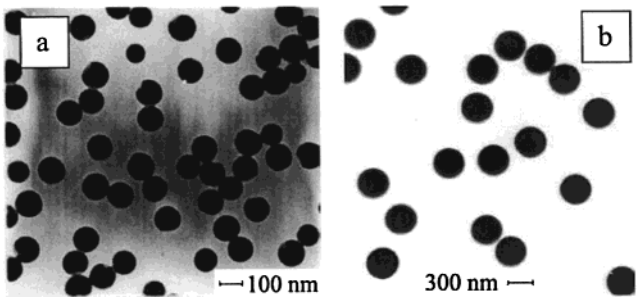

Figure 3. TEM micrographs of samples 6MDS (a) and 6S (b).

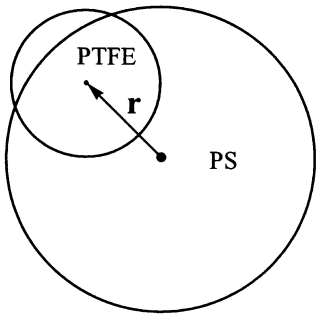

Figure 4. Schematic representation of the hemispherical morphology of the PTFE−PS core−shell nanospheres.

lighter spot, deriving from the PTFE seed, which is not fully embedded into the PS shell. Consequently, the nanosphere morphology appears slightly hemispherical (Figure 4). Similar morphologies are theoretically predicted starting from thermodynamic considerations[15,16] of the behavior of two immiscible oils in water, which is directed by the various interfacial tensions and spreading coefficients, and were observed in a variety of systems and conditions.[17−19] However, this morphology is at variance with respect to the one reported[12,13] for particles consisting of PTFE and cross-linked polybutadiene shell and PTFE and cross-linked PS. In these cases, a perfect core−shell morphology was observed. This difference could derive from the smaller size of the PTFE seeds employed in the present study or to the surfactant mixture and concentration which are known[18] to substantially affect the core−shell morphology.

The TEM micrographs of the entire *n*MDS series is reported in Figure 5. The nanosphere size decreases as the amount of PTFE seed increases but a slight increase

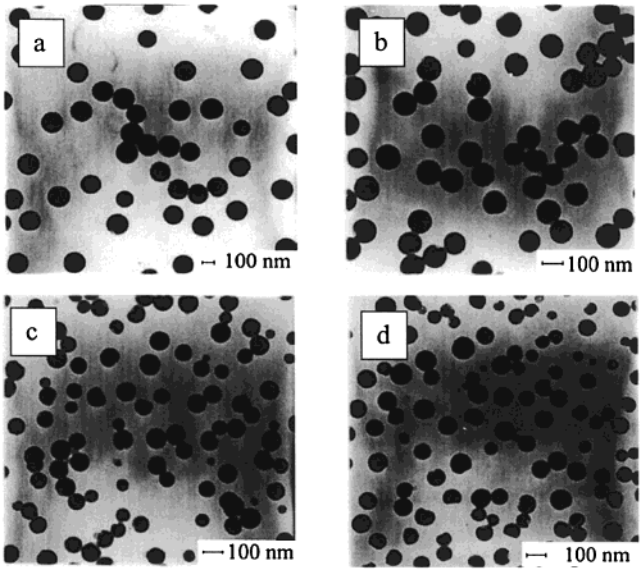

Figure 5. TEM micrographs of the *n*MDS sample series: 3MDS (a), 6MDS (b), 12MDS (c), and 18MDS (d).

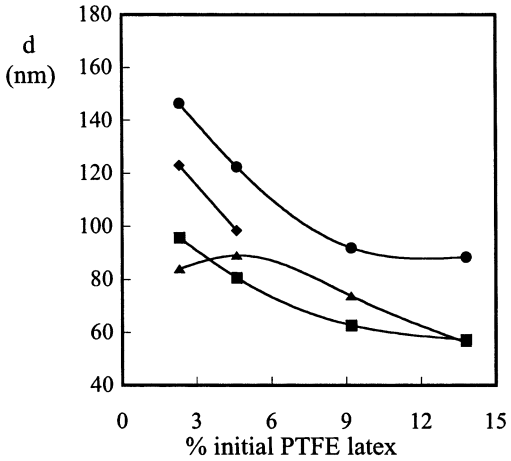

Figure 6. Trend of the particle diameter in the various sample series as a function of the amount of initially added PTFE: *n*MDS, ●; *n*MDdS, ◆; *n*DV2S, ▲; *n*DV2dS, ■.

in the size distribution can be noticed on going from sample 3MDS to sample 18MDS. The hemispherical morphology is always observed, not only for sample series *n*MDS but also for all the other samples including those prepared starting from DV3 latex, which consists of rodlike particles.

Table 3 collects the diameter values, including the standard deviations, for all the prepared samples. Diameters ranging from 146 to 56 nm and standard deviations from 6 to 10 nm are observed. In all the series, the particle diameter decreases steeply at first and then more gradually as the initial PTFE amount increases (Figure 6). The same decreasing trend is observed for PS sample series *n*S (Table 3).

The ζ potential of the various samples was also measured and were observed to be between −29 and −67 mV. Negative ζ potentials indicate that the latexes are stabilized by electrostatic repulsions of negative charges at the particles surface. The negative charges derive from both the residual surfactant from the PTFE synthesis and the ionic initiator fragments.

To obtain information about the molar mass and molar mass distribution, in sample series *n*MDS the polystyrene was separated from PTFE through addition

Table 3. Size, ζ Potential, and Composition of the Samples Derived from Different Techniques

sample	*d*(TEM) (nm)	*d*(PCS) (nm)	ζ potential (mV)	theoretical comp (%)	TEM comp (%)	PCS comp (%)	DSC comp (%)	TGA comp (%)
MD		41 ± 1.5						
DV2		33 ± 2.5						
3MDS	146.4	138.8 ± 1.2	−51.8 ± 1.1	5.2	4.5	5.5	4.3	5.2
6MDS	122.5	112.8 ± 0.6	−43.4 ± 3.5	9.8	7.6	9.7	7.9	6.7
12MDS	92	91.9 ± 0.6	−40.1 ± 1.7	17.9	17.6	17.3	16.8	19.4
18MDS	88.5	89.2 ± 0.6	−45.4 ± 1.3	24.5	19.2	18.9	24.5	22.7
3MDdS	123	129.4 ± 1.9	−50.4 ± 0.3	5.86	7.6	6.6	7.0	8.8
6MDdS	98.4	114.1 ± 0.7	−47.4 ± 1.2	11.1	14.4	9.5	12.7	13.8
3DV2S	84	95.7 ± 1.1	−44.9 ± 2.6	6.1	16	11.6	5.6	6.7
6DV2S	89	90.4 ± 1.4	−43.2 ± 2.9	11.5	14.3	13.6	10.7	8.7
12DV2S	73	72.8 ± 0.4	−29.4 ± 2.9	20.8	24.3	24.5	19.2	19.4
18DV2S	56	68.5 ± 0.4	−45.3 ± 1.2	27.9	46.5	28.7	31.4	29.5
3DV2dS	95.9	97.9 ± 1.0	−46.8 ± 0.9	6.3	11.5	10.9	6.5	6.5
6DV2dS	80.7	84.9 ± 0.5	−45.6 ± 0.5	11.8	18.6	16.2	11.3	12.3
12DV2dS	62.8	65.6 ± 0.6	−45.4 ± 5.6	21.1	35.5	25.2	25	21.8
18DV2dS	57.3	72.0 ± 0.9	−58.9 ± 3.4	28.8	44	31.9	35.6	30.11
3DV3S	112.8	115.1 ± 1.4	−47.3 ± 1.2	7.3	8.5	6.5	7.9	7.0
3S	396.9	376.1 ± 3.4	−67.4 ± 0.6					
6S	358.8	309.8 ± 2.8	−66.0 ± 0.7					
12S	305.2	286.6 ± 2.5	−65.0 ± 0.8					
18S	232.2	212.6 ± 1.2	−62.7 ± 0.7					

of THF to the core−shell sample and centrifugation at 18 000 rpm. Under these conditions, quantitative sedimentation of PTFE was obtained, and the polystyrene was recovered from the supernatant. The molar mass data of the polystyrene component in the *n*MDS core−shell nanoparticles were determined by SEC and result in $M_n = 1.77 \times 10^5$ and $M_w/M_n = 4.7$ for 3MDS, $M_n = 1.91 \times 10^5$ and $M_w/M_n = 5.0$ for 6MDS, $M_n = 2.28 \times 10^5$ and $M_w/M_n = 5.2$ for 12MDS, and 3.81×10^5 and $M_w/M_n = 5.5$ for 18MDS. Both M_n and M_w increase slightly as the amount of the feed MD seed in the polymerization reaction increases. This effect is clearly due to the increase in the number of polymerization loci.[20]

The nanosphere composition was determined by several techniques. Provided that no pure PS or PTFE nanospheres are present, the composition of the core−shell nanospheres was calculated from the amount of the initially added PTFE and styrene, taking into account the relevant polymer densities and the nanosphere yield. These calculated composition data can be compared to the experimentally determined values deriving from TEM and PCS. In these cases, the composition was derived from the PTFE seed size and from the densities of the PTFE and PS assuming the presence of core−shell nanospheres only. In addition, the composition can be also estimated from thermogravimetric (TGA) analysis and, under appropriate hypotheses, from differential scanning calorimetry (DSC).

As typical examples, Figures 7 and 8 report the TGA and DSC second heating curves of *n*MDS sample series. For comparison, the TGA and DSC curves of latex MD and the TGA curve of a purely PS sample are included. As the weight losses at 360 and 500 °C are clearly assignable to PS and PTFE decomposition, respectively, it is evident that the PTFE weight loss increases proportionally to the initially added PTFE. In a somewhat parallel fashion, in the DSC curves of *n*MDS sample series an endothermic peak at about 323 °C, corresponding to PTFE melting and a step due to the PS glass transition at 104−105 °C are observed. The melting temperature of PTFE is constant whereas a slight increase in the PS glass transition temperature is observed as the series is ascended. However, the glass transition temperature of the polystyrene samples

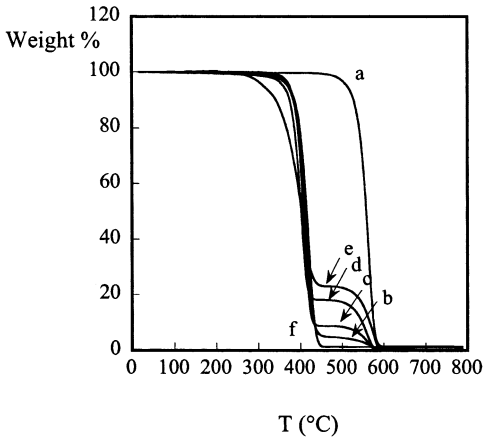

Figure 7. TGA curves at 10 °C/min heating rate for various samples: MD (a), 3MDS (b), 6MDS (c), 12MDS (d), 18MDS (e), and 6S (f).

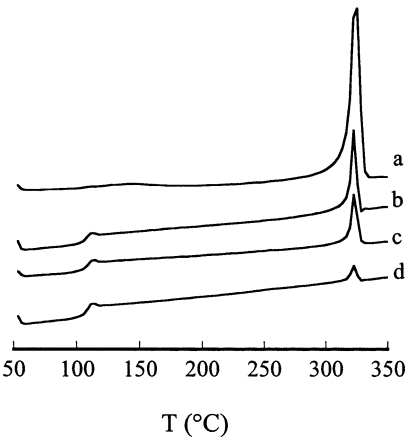

Figure 8. DSC second heating curves of *n*MDS sample series at 10 °C/min heating rate: MD (a), 12MDS (b), 6MDS (c), and 3MDS (d).

recovered from the core−shell nanospheres is equal to the one of the polystyrene shell in the corresponding core−shell sample. Consequently, the temperature increase should be ascribed to the parallel increase[21] in the polystyrene molar mass along the series (see above). This indicates that the PTFE and PS phases within the core−shell structure do not strongly interact. Conse-

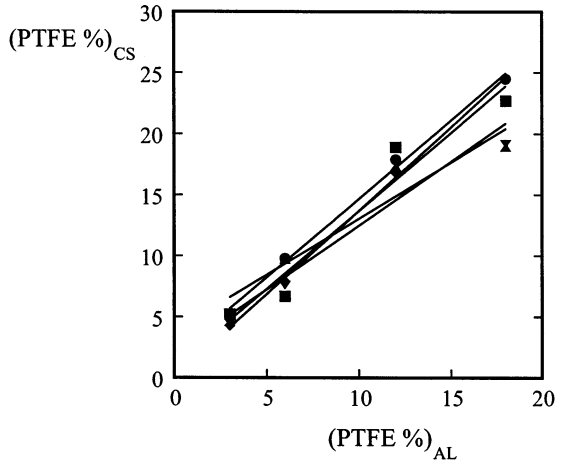

Figure 9. Composition data of the *n*MDS nanosphere series estimated and calculated using various techniques as a function of the amount of initially added PTFE: (●) calculated; (■) TGA; (◆) DSC; (▲) PCS; (▼) TEM.

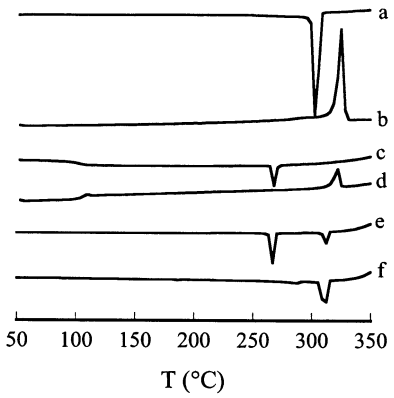

Figure 10. DSC curves at 10 °C/min: MD heating and cooling (a and b); 3MDS heating and cooling (c and d); bMDS1 cooling (f); bMDS2 cooling (e).

quently, it appears correct to evaluate from the PTFE melting enthalpy the amount of PTFE and, by difference, the amount of PS. This calculation was performed on all the samples, and the determined composition can be compared with the one estimated by the other techniques (Table 3). Figure 9 reports collectively the composition data of the *n*MDS series estimated and calculated using the above techniques as a function of the amount of initially added PTFE. The various composition curves nearly coincide with one another and are in excellent agreement with the theoretically predicted one. A similar behavior is observed also for the other sample series; this further confirms the low, if any, interaction between the PTFE core and the PS shell.

The overall picture of these data indicates that the composition or conversely the nanosphere size can be precisely tuned by appropriately adjusting the ratio between the initially added PTFE seed and styrene.

However, a peculiar thermal behavior was also observed during the DSC analysis. For the PTFE sample MD alone, the crystallization process occurs at 305 °C (Figure 10a), in agreement with literature data,[22] whereas, in the case of the core−shell nanospheres, the crystallization exotherm is observed at 270 °C (Figure 10c). This temperature does not depend on the core−shell composition. The same effect is observed also in the other sample series. For example, the crystallization of the PTFE sample DV2 is 312 °C whereas the

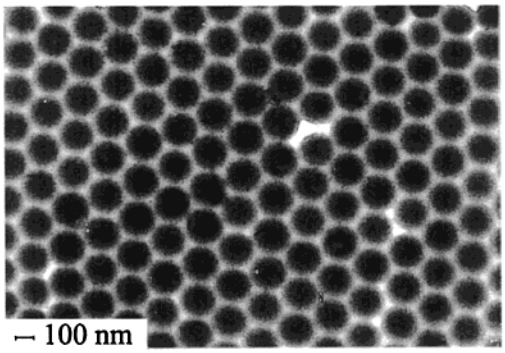

Figure 11. TEM image of a well-ordered two-dimensional array of nanospheres obtained by deposition from methanol.

crystallization of PTFE in sample series *n*DV2S occurs at 270 °C.

To understand the crystallization behavior of PTFE under various conditions, two blends were prepared. Blend bMDS1 was obtained by mechanically mixing PS powder sample 12S with 5% (w/w) of MD powder, whereas blend bMDS2 was obtained by mixing the corresponding 12S latex and MD latex in the same solid weight percent and evaporating the water. In the DSC cooling curve of blend bMDS1 (Figure 10f), the PTFE crystallization exotherm is observed at 305 °C whereas in the case of blend bMDS2, two crystallization exotherms are observed centered at 305 and at 270 °C (Figure 10e). The striking difference in the crystallization behavior between the two blends clearly reflects the difference in the degree of particle interdispersion which is obviously higher in the case of blend bMDS2. Consequently, the dual crystallization behavior of PTFE can be ascribed to both the restricted size of the PTFE material, once in the form of individual core embedded within a PS shell or matrix, and/or to unfavorable boundary conditions, provided by PS shell or matrix, to the PTFE crystallization.

A final remark concerning the internal structure of the material, as obtained through three-dimensional structuring and annealing the above core−shell nanosphere samples, should be made. The various core−shell nanosphere samples are sufficiently regular to be built into a well-ordered two-dimensional array as illustrated in Figure 11, which reports the TEM image of sample 3MDS after deposition from methanol, and potentially into a three-dimensional array through appropriate shaping techniques.

However, their peculiar hemispherical morphology does not allow nanocomposite to be obtained in which the PTFE cores are placed into regular registry (Figure 12a).

In fact, the orientations of the vectors connecting the center of the nanospheres to the center of their respective cores are not correlated to one another even though the nanospheres are placed into a three-dimensional well-ordered array. Indeed, there are also some constraints due to the presence of PS which should be taken into account. Certain space regions are not available to the PTFE cores, as illustrated in Figure 12b. In addition, only clusters with a maximum of four PTFE cores are allowed. There restrictions lead to a nonrandom distribution of PTFE within the final nanocomposite.

A preliminar dynamic-mechanical investigation was also performed on sample series *n*MDS in the linear viscoelasticity region at the frequency of 1 Hz, between 40 °C and the temperature at which the samples lost

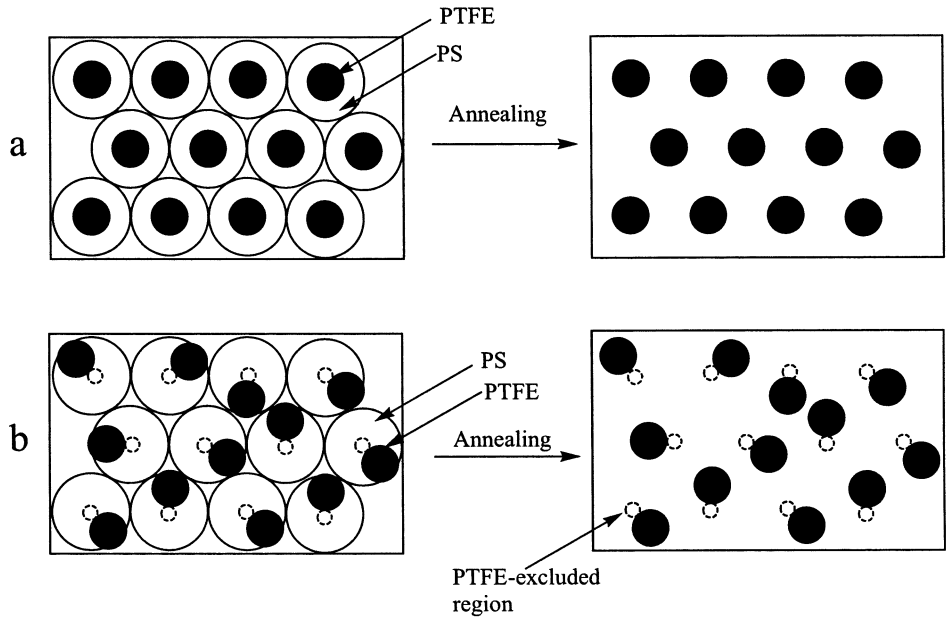

Figure 12. Schematic representation of the nanocomposite structure after three-dimensional nanosphere assembly and thermal treatment starting from regular core−shell nanospheres (a) and hemispherical core−shell nanospheres (b).

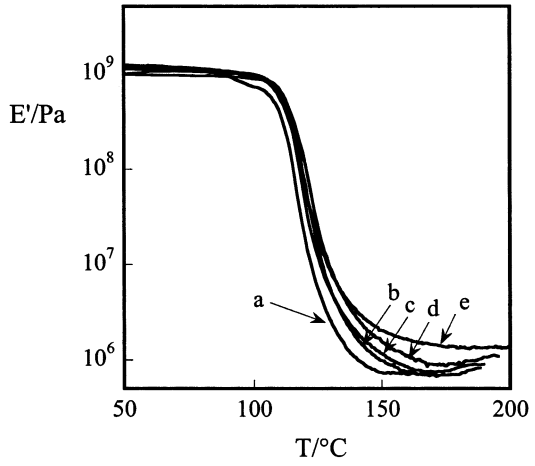

Figure 13. Trend of the storage modulus E' for *n*MDS sample series and a PS sample as a function of temperature: 6S (a), 3MDS (b), 6MDS (c), 12MDS (d) and 18MDS (e).

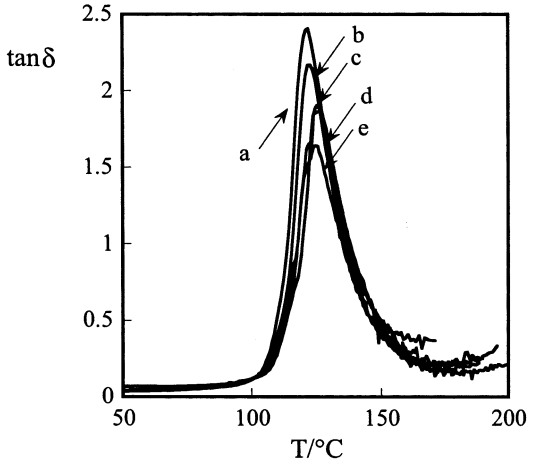

Figure 14. Trend of the loss tangent for *n*MDS sample series and a PS sample as a function of temperature: 6S (a), 3MDS (b), 6MDS (c), 12MDS (d), and 18MDS (e).

their dimensional stability, with a heating rate of 4 °C/min. The samples for the dynamic-mechanical analysis were prepared simply by hot pressing the powder polymer sample into a rectangular mold at 160 °C for 20 min. No structural ordering was attempted. Figures 13 and 14 illustrate the trends of the storage modulus E' and tan δ, respectively, as a function of the temperature.

In addition, the same figures report the relevant curves for a PS sample. The dynamic storage modulus E', which is about 1.5×10^9 Pa at 60 °C for PS but is higher for the *n*MDS samples, decreases with increasing temperature with a drop at about 115 °C, corresponding to the glass transition of the PS component. At temperature above the glass transition, the PS plateau modulus increases as the PTFE amount in the sample increases. A parallel decrease in the dumping is observed, as expected for composites based on rigid fillers.[23] However, the temperature of the glass transition of the polystyrene component is not affected by the PTFE amount and only a small broadening of the relaxation process in the high-temperature portion of the transition occurs thus further indicating negligible interfacial effects between the PS and PTFE components.

Conclusion

PTFE latexes with particles in the submicrometer size range, were employed as seeds in the emulsifier-free styrene emulsion polymerization. Although poor colloidal stability was observed in some latexes, leading to coalescence immediately after the beginning of the polymerization, stable latexes were generally obtained. No residual PTFE nor secondary nucleation was observed, thus leading to PTFE−PS core−shell latexes. By appropriately choosing the ratio between the styrene monomer and the PTFE seed in the reaction mixture, it is possible to obtain particles with predetermined size and narrow size distribution. In all cases, a slightly hemispherical morphology was observed. PTFE and PS phases do not strongly interact. However, peculiar effects related to the high degree of segregation of PTFE cores and their small size, and possibly to the PTFE/PS interface, were observed.

Accordingly, the above core−shell nanoparticles represent a novel class of highly specific but very efficient PTFE-based additives capable of being perfectly dispersed into PS and PS-miscible polymer matrices as well. In addition, although their peculiar morphology prevents, to some extent, the formation of perfectly ordered nanocomposites, nanostructures with nonrandom distribution of PTFE can be still obtained.

References and Notes

(1) Feiring, A. E.; Imbalzano, J. F.; Kerbow, D. L. *Plast. Eng.* **1994**, 27.
(2) Scheirs, J. *Modern Fluoropolymers*; Wiley: New York, 1997.
(3) Siperko, L. M.; Thomas, R. R. J. *Adhesion Sci. Technol.* **1989**, *3*, 157.
(4) Ishizu, K. *Prog. Polym. Sci.* **1998**, *23*, 1383; Zhao, C. L.; Roser, J.; Heckmann, W.; Zosel, A.; Wistuba, E. *Prog. Org. Coat.* **1999**, *35*, 265. Kalinina, O.; Kumacheva, E. *Chem. Mater.* **2001**, *13*, 35.
(5) Beecroft, L. L.; Ober, C. K. *Chem. Mater.* **1997**, *9*, 1302.
(6) Shen, Y.; Friends, C. S.; Jiang, Y.; Jakubczyk, D.; Swiatkiewicz, J.; Prasad, P. N. *J. Phys. Chem.* **2000**, *104*, 7577.
(7) Giannetti, E.; Visca, M. US Patent 4 864 006, 1987.
(8) Kapeliouchko, V.; Marchese, E.; Colaianna, P. EU Patent Application 969027.
(9) Gozzi, G. US Patent 4 632 963 1987.
(10) Albano, M.; Apostolo, M.; Arcella, V.; Marchese, E. US Patent 6 395 834 2002.
(11) Roma, P.; Camino, G.; Luda, M. P. *Fire Mater.* **1997**, *21*, 199.
(12) Okaniwa, M. *J. Appl. Polym. Sci.* **1998**, *68*, 185.
(13) Othegraven, J.; Piazza, R.; Bartsch, E. *Macromol. Symp.* **2000**, *151*, 515.
(14) Kipp, B. E.; DeSimone, J. M.; Pochan, D. J.; Gido, S. P. *Abstr. Prepr. Am Chem. Soc.* **1997**, *213*, 31.
(15) Torza, S.; Mason, S. *J. Colloid Interface Sci.* **1970**, *33*, 67.
(16) Sundberg, D. C.; Casassa, A. P.; Pantazopoulos, J.; Muscato, M. R. *J. Appl. Polym. Sci.* **1990**, *41*, 1425.
(17) Cho, I.; Lee, K. W. J. *Appl. Polym. Sci.* **1985**, *30*, 1903.
(18) Chen, Y. C.; Dimonie, V.; El-Aasser, M. S. *J. Appl. Polym. Sci.* **1991**, *42*, 1049.
(19) Xu, M.; Peterson, D. S.; Rohr, T.; Svec, F.; Fréchet, J. M. J. *Anal. Chem.* **2003**, *75*, 1011.
(20) Gilbert, R. J. *Emulsion Polymerization: A Mechanistic Approach*; Academic Press: London, 1995.
(21) Lijia, A.; Dayong, H.; Jiaokai, J.; Zhigang, W.; Donghong, Y.; Bingzheng, J.; Zhenhua, J.; Rongtang, M. *Eur. Polym. J.* **1997**, *33*, 1523.
(22) Wang, X. Q.; Chen, D. R.; Han, J. C.; Du, Y. D. *J. Appl. Polym. Sci.* **2002**, *83*, 990.
(23) Nielsen, L. E.; Landel, R. W. *Mechanical Properties of Polymers and Composites*; Marcel Dekker: New York, 1994.

MA0259970